

Bi-phase age-related brain gray matter magnetic resonance T1 ρ relaxation time change in adults

^{1*}Yáo T Li *BSc*, ^{2*}Hua Huang *MMed*, ³Zhizheng Zhuo *PhD*, ²Pu-Xuan Lu *MB*, ¹Weitian Chen *PhD*, and ¹Yì Xiáng J Wáng *MMed, PhD*

1. Department of Imaging and Interventional Radiology, Faculty of Medicine, The Chinese University of Hong Kong, Prince of Wales Hospital, Shatin, New Territories, Hong Kong SAR
2. Department of Radiology, Shenzhen No. 3 People's Hospital, Shenzhen, Guangdong Province, People's Republic of China.
3. MR Clinical Sciences, Philips Healthcare Greater China, Beijing, People's Republic of China.

* These two authors contributed equally to the work.

Address correspondence to: Dr Yì Xiáng J Wáng
E-mail: yixiang_wang@cuhk.edu.hk

Running title:
Age-related brain T1 ρ change

Abstract

Objectives: To investigate normative value and age-related change of brain magnetic resonance T1 ρ relaxation at 1.5T.

Methods: 20 males (age: 40.7 \pm 15.5 years, range: 22-68years) and 22 females (age: 38.5 \pm 14.8 years, range: 21-62 years), were scanned at 1.5 Tesla using 3D fluid suppressed turbo spin echo sequence. Regions-of-interests (ROIs) were obtained by atlas-based tissue segmentation and T1 ρ was calculated by fitting the mean value to mono-exponential model. Correlation between T1 ρ relaxation of brain gray matter regions and age was investigated.

Results: A regional difference among individual gray matter areas was noted; with hippocampus (98.37 \pm 5.37 msec) and amygdala (94.95 \pm 4.34 msec) have the highest measurement, while pallidum (83.81 \pm 5.49) and putamen (83.93 \pm 4.76) the lowest measurement. T1 ρ values decreased slowly (mean slope: -0.256) and significantly (p <0.05) with age in gray matter for subjects younger than 40 years old, while for subjects older than 40 years old there was no significant correlation between T1 ρ relaxation and age.

Conclusion: T1 ρ relaxation demonstrates a bi-phase change with age in adults of 22-68 years.

Key words: Magnetic Resonance Imaging, T1 ρ relaxation; Brain; Age

Introduction

Matter magnetic T1 ρ relaxation has the potential to provide information about the low frequency motions (100Hz to a few kilohertz) in biological systems [1, 2]. T1 ρ relaxation not only depends on T1 and T2 but also has contributions from several MR interactions such as chemical exchange, dipolar interaction and J-coupling. Depending upon the tissue type, more than one mechanism may be operative simultaneously but with different relative contributions. During recent years, T1 ρ relaxation has been increasingly used to explore the pathophysiology or predictive diagnostics of a number of neurological conditions [4-10]. Previous studies suggested that neurodegeneration may contribute to the increased T1 ρ in brain regions [11-13]. For example, cerebral atrophy, which reflects underlying neuronal loss, has been reported to be associated with the increased T1 ρ values in the hippocampus and medial temporal lobe of Alzheimer's disease [11]. Although the biophysical/biochemical mechanism remains to be further investigated, novel MRI techniques such as T1 ρ , T1 ρ dispersion, chemical exchange saturation transfer and its variant chemical exchange imaging with spin-lock technique may provide early imaging biomarkers for neurodegeneration diseases including Alzheimer's disease, Parkinson's disease and dementia [14-18]. These techniques have been refined to be increasingly more time-efficient, faster and more robust in recently years [19-30].

T2 relaxation has also been explored as one of the contrast mechanism in disease characterization [31, 32]. The relationship between T2 relaxation and physiological ageing remains not confirmed yet. Siemonsen *et al* [33] studied 50 subjects (age: 12–91 years) and found an increase in T2 that linearly correlated with age in the thalamus and three white matter structures, but not in the caudate nucleus and lentiform nucleus. Ding *et al* [34] studied 70 normal subjects (age: 3 weeks-31 years) and showed that T2 decreased with increasing age; the rate of decrease was greater at a younger age and

slower in the years after, indicating a nonlinear relationship with age. Hasan *et al* [35] studied 130 healthy subjects (age: 15–59 years) and reported the relation between T2 and age in whole brain gray and white matter, caudate nucleus, and the anterior limb of internal capsule followed a quadratic, U-shaped curve. More recently, Wang *et al.* [36] studied 77 normal subjects (age: 9-85 years) and reported brain tissue R2 (1/T2)-age correlations followed various time courses with both linear and nonlinear characteristics depending on the particular brain structure.

T1 ρ -age relationship has not been studied as much as T2 relaxation. Borthakur *et al* [37] found no relationship between T1 ρ vs. age in 16 elderly subjects (age: 70-91 years). Recently Watts *et al* [38] studied 41 subjects (age: 18-76 years) and reported T1 ρ values significantly decrease with age in cortical gray matter, left and right caudate, putamen, hippocampus, amygdala, and nucleus accumbens; while increases with age were observed in white matter tracts. Information on age-related change in T1 ρ relaxation is not only needed to gain a deeper understanding of brain ageing but also useful as a normative data set for examinations performed with T1 ρ MRI in patients. The primary goal of this study was to further clarify the discrepancy seen in the reported literature [37, 38].

Materials and Methods

Subjects

This study was approved by the local ethical committee. There were 42 adults volunteers, including 20 males (ages 22-68 years, with a mean and standard deviation of 41 \pm 16 years) and 22 females (ages 21–62 years, with a mean and standard deviation of 39 \pm 15 years). None of the subjects had neurological diseases except those generally associated with ageing in older subjects [39].

MRI protocol

The MRI data sets were acquired with a 1.5 T Philips Achieva scanner (Philips Healthcare, Best, the Netherlands) using a 16 channel head coil (Invivo Corp, Gainesville, USA). The pulse sequence was similar to that used in [38]. The T1 ρ -weighted images were acquired using 3D fluid suppressed turbo spin echo (TSE) sequence. A combination of T2-preparation and inversion recovery was used for fluid suppression, which was equivalent to the fluid suppression method reported by Wong *et al* [40]. Adiabatic refocusing and inversion pulses were used for T2-preparation and the 180⁰ inversion respectively, to improve the robustness against B₁ inhomogeneity. The TI (time of inversion) used for fluid suppression was 1650msec. The spin-lock was achieved using a rotary echo approach as described by Charagundla *et al* [41]. Six T1 ρ -weighted images were acquired with total spin lock time (TSL) 0, 20, 40, 60, 80, and 100msec. After T1 ρ -prep, the imaging sequence consists of a 3D TSE sequence with variable flip angle. The imaging parameters include: sagittal plane, FOV 25cm x 25cm, TR/TE 4800/228ms, 3D isotropic resolution 1.8x1.8x1.8mm³, 100 slices with whole brain coverage, TSE factor 182 with echo spacing 2.3msec, SENSE acceleration factor 2.6 along anterior-posterior and 2 along right-left direction, and NSA 2. The acquisition time of each spin lock time was 1 min 50 s, giving a total acquisition time about 7min 30sec.

Data Analysis

In order to achieve the brain motion-correction for all the images with different TSLs caused by involuntary brain movement, respiration and CSF pulsation, all the T1 ρ images with different TSLs were realigned to the first T1 ρ image (TSL=0). The individual T1 ρ image with TSL=0 was segmented into gray matter and white matter by using a series of Tissue Probability Maps (TPM) templates in MNI Montreal Neurological Institute space using SPM8 (Functional Imaging Laboratory, The Wellcome Trust Center for NeuroImaging, Institute of Neurology, UCL University College London, London, UK) [42]. Tissue Probability Maps assign voxels a probability of belonging to gray matter or white matter or CSF or other tissues. The subject-specific segmented gray matter and white matter images in original T1 ρ image (native space) were gray matter (GM) and

white matter (WM) distribution probability mapping with a range of 0-1. The individual gray and white matter binary masks, i.e. images with only 0 and 1 values, were obtained by thresholding the segmented images with a threshold of 0.5. For acquiring gray matter binary masks, the voxels were defined belonging to gray matter if the probability was higher than 0.5, and voxel value was set to 1 if probability was higher than 0.5 and otherwise voxel value was set to 0; and the same was applied to white matter binary masks [38, 43-45].

The individual gray and white matter binary masks were applied on the original T1 ρ images with different TSLs to extract the gray matter and white matter [38]. Optimized atlas-based methods provide more accurate and specific diagnostic surrogate markers compared to whole brain histograms, voxel-by-voxel or large ROI methods. Specific region-of-interests (ROIs) such as hippocampus were extracted based on the Anatomical Automatic Labeling template (in MNI Montreal Neurological Institute space) by using REST software (Resting-State fMRI Data Analysis Toolkit, State Key Laboratory of Cognitive Neuroscience and Learning, Beijing Normal University, Beijing, China) [46]. All the original T1 ρ images were normalized to the MNI space by using the normalization parameters generated in New Segment batch in SPM8. In this way, all the T1 ρ images were warped into the MNI space same as ROI masks. Finally, the ROI masks were applied on the normalized T1 ρ images to calculate the T1 ρ values within specific ROIs. The segmentation results were visually verified by an experienced radiologist.

The T1 ρ -weighted images are assumed to follow a mono-exponential decay model:

$$I(\text{SLT}) = I_0 \times \exp(-\text{SLT}/T1\rho) \quad [1]$$

Where I_0 is the image when SLT is zero. To avoid potential measurement bias due to relative lower SNR at 1.5T (supplement document 1), after signal averaging within ROI, non-linear least square fit with the Levenberg-Marquardt algorithm was used to fit the

data to the mono-exponential model. All image analyses were conducted in Matlab (MathWorks Inc, USA). Weighted least square was used to assess fitting quality. When poor fitting data ($R^2 < 0.95$) occurred, possible error was checked again. Points with value $> (\text{mean} + 2\text{SD})$ or $< (\text{mean} - 2\text{SD})$ were discarded.

Statistical Analysis

All statistical analyses were performed with software SPSS22 (IBM Corp, Chicago, USA). Two-tailed Student t-test, which was validated using a Kolmogorov-Smirnov test for normality, was used to check the difference between T1 ρ values of male and female, left and right brain. Despite the generally existing cerebral asymmetry [47], no asymmetry in MR relaxivity asymmetry has been reported between the left and right sides of the brain as well as no difference between males and females [36, 38, 40, 49], and our data analysis showed the same. Therefore the T1 ρ values from two hemispheres were averaged for analysis.

Based on the initial visual inspection of the trend of T1 ρ vs. age, and our polynomial fitting showed the lowest T1 ρ value during the age period 43 to 54 years (supplement document 2), and plus with reference to data presented by Hasan *et al* [35] and Wang *et al* [36], the data in this study were divided into two groups, i.e. before 40 years group ($n=22$, 11 males and 11 females) and after 40 years group ($n=20$, 9 males and 11 females). Then linear regression and Pearson correlation coefficients between T1 ρ values and age were calculated. Analysis of variance (ANOVA) with repeated measures and multiple comparisons were used to compare the T1 ρ variation among different tissue regions.

Results

Table 1, 2 showed the mean, standard deviation (SD), Pearson correlation coefficient and p-value of gray matter and specific structures for subjects younger than 40 years and older than 40 years, respectively. In subjects younger than 40 years, T1 ρ values in

the selected gray matters showed significant negative correlation with age. However, for subjects older than 40 years, T1 ρ values in the selected gray matters showed no significant correlation with age (Figure 1). Supplement document 3 shows if subjects of all age are grouped together for linear regression fit, the correlation is much reduced compared with younger subjects only (< 40 years).

Analysis of variance (ANOVA) with repeated measures showed T1 ρ values varied in different gray matter structures (Figure 2), with Amygdala and Hippocampus had the highest mean T1 ρ values of 94.95 \pm 4.34 msec and 98.37 \pm 5.37 msec, and putamen and pallidum had the lowest mean T1 ρ values of 83.81 \pm 5.49 msec and 83.93 \pm 4.76msec.

Global white matter measured T1 ρ value of 88.65 \pm 3.47 msec, and the association with age was not significant ($p=0.18$, Supplement document 3).

Discussion

The diagnosis and therapy of age-related chronic diseases will become more and more challenging in the course of the next few decades because the percentage of elderly people is increasing. Objective and quantitative imaging strategies sensitive to early biochemical changes in brain tissue will benefit evaluation of potential new therapies and longitudinal monitoring of disease progression. In a pre-clinical study Plaschke *et al* [50] demonstrated MR Relaxometry may shows subtle changes not detected by neuropathological evaluations. If T1 ρ imaging is to have application to neurodegenerative disease and other pathology, it is essential to understand its variation during normal aging and normative values for T1 ρ across different ages.

T1 ρ relaxation time constant is influenced by molecular processes that occur in the millisecond range, such as chemical exchange of protons between water associated with macromolecules and free water. In biological tissues, T1 ρ is dependent on the macromolecular composition. Studies on the relationship between T1 ρ and ageing are

till now limited. Watts *et al*'s study at 3T estimated brain gray matter T1 ρ values of 74 msec to 86 msec [36]. Further, Gonyea *et al* [4] reported normal appearing gray matter had T1 ρ of 78.2 ± 1.3 msec. The gray matter mean T1 ρ value measured in the current study ranged from 83.76 msec to 96.00 msec, which is longer than the data presented by Watts *et al* [36] and Gonyea *et al* [4]. On the other hand, the regional variation in our study is similar to Watts *et al* [36], where the amygdale and hippocampus also had the highest mean T1 ρ values and putamen and pallidum had lowest mean T1 ρ values, though this point was not specified in their report. One plausible explanation would be these regional T1 ρ measurements were due to local iron deposition difference as discussed in Vymazal *et al*'s paper on T2 relaxivity [31]. Our measurements broadly agree with earlier reports at 1.5T. Borthakur *et al* [37] reported T1 ρ values (1.5T) for gray matter of 86.4 ± 4.4 msec in their elderly control subjects (age 78 ± 2 years). Haris *et al* [12] reported T1 ρ values (1.5T) in the left and right hippocampus of 90.2 ± 12.3 and 92.2 ± 13.6 ms respectively in a control group aged 71.2 ± 9.8 years. T1 ρ has higher value at 1.5T than at 3T supports the biophysics of T1 ρ relaxation mechanism [1,2].

The T1 ρ and T2 values are correlated with T2 can be regarded as a special case of T1 ρ with a spin lock frequency of 0 Hz. It was reported at the spin lock frequency around 500 Hz, T1 ρ provides additional sensitivity to low frequency processes [2, 4]. Recently, Wang *et al* [36] reported significant positive correlation between tissue R2 and age from 9 to 30 years old in gray matter structures; however, the R2-age correlation after age 40 demonstrated more diverse characteristics. Hasan *et al* [35] reported a quadratic relationship between global T2-values for gray matter with a minimum around age 45. Watts *et al* [38] reported a decrease of gray matter T1 ρ with age. The inspection of our data suggested T1 ρ of gray matter might follow a bi-phase change relative to age. The initial decreasing phase was till around 40 years old, while gray matter in subjects older than 40 years old showed no clear age relationship. We argue that a further look at Watts *et al*'s data may also suggest there was no apparent trend in subjects older than 40 years as well (Fig 2 of reference 38). The decreasing trend was mainly contributed by

subjects younger than 40 years [38], and the same might be true with Hasan *et al*'s T2 relaxation results (Fig 5 of reference 35). Our results would also agree with the initial study of Borthakur *et al* [37], where no relationship was found between age and T1 ρ in elderly subjects. Note if a polynomial fitting approach is taken, the fitting-line on right-side is more likely showing a U-turn toward up than being fitted flat (supplementary Fig 2, Fig 5 of reference 35). Our study further demonstrates the sophisticated manner of the relationship of MR relaxation vs. age increase. It can be nonlinear, and also vary across brain regions [36]. The comforting side would be that no clear change associated with ageing was noted for subjects older than 40 years. We would like to suspect even more older subjects were recruited and a type of change pattern reaches statistical significance, this correlation will remain weak. Considering the physiological life span of human beings (\sim 100 years), the biochemical process related to a decreasing T1 ρ value before 40 years old is more likely related to maturation than to ageing.

Recently, Zhao *et al* [51] reported a T1 ρ increase associated with ageing (\sim 15 months) in rat brain gray matter areas of the thalamus, hippocampus and frontal cortical regions. This trend apparently differs from the results from the current study. However, Plaschke *et al* [50] also found a significant increase in T2 relaxation time in senescent (18-month-old) rats' brain compared with the same rats measuring at the age of 12 month, with the value for hippocampus increased from 77.2 ± 29 to 110 ± 28 msec (2.35-T B0 magnetic field). T2 relaxation time was specially increased after systemic hypotension treatment. Importantly, Plaschke *et al* showed increased T2 relaxation time in rat brain was negatively correlated with reference memory. In addition to biological differences between human brains and rodent brains and different relative ages, the bi-phase or a quadratic curve of brain tissue relaxivity changes may partially explain the T1 ρ divergence in this study and the results of Zhao *et al* [35, 36, 51].

There are a few limitations for this study. The number of study subject remains relatively small. Both children and very old subjects were not included in this study. The

conclusion of age-dependant change in subjects older than 40 years cannot be firmly drawn from this study. The subjects were adjudged to be healthy based on that there were no specific neurological symptoms, and the MRI reading being normal except changes commonly seen in elderly subject [39]. We could not exclude the possibility that a few subjects had un-diagnosed psychiatry diseases. However, this would be a potential limitation for all similar studies, and it is unlikely this would change the conclusion of this study.

In conclusion, our study indicates the complexity of age-related T1 ρ changes in the brain as the changes do not necessarily follow a linear pattern, and also can be structure specific. Careful observation suggests consistent patterns from multiple studies which have been published recently, with adults of aged <40 years demonstrating decreasing T1 ρ relaxation correlated with age. Brain tissue T1 ρ measurement at 1.5T is slightly longer than at 3T which supports the biophysics of T1 ρ relaxation.

Acknowledgement:

We thank Queenie Chan PhD, Philips Healthcare Greater China, for her supports during the study.

References:

1. Gilani IA, Sepponen R. Quantitative rotating frame relaxometry methods in MRI. *NMR Biomed.* 2016;29(6):841-61.
2. Wáng YX, Zhang Q, Li X, Chen W, Ahuja A, Yuan J. T1 ρ magnetic resonance: basic physics principles and applications in knee and intervertebral disc imaging. *Quant Imaging Med Surg* 2015;5(6):858-885.
3. Hulvershorn J, Borthakur A, Bloy L, Gualtieri EE, Reddy R, Leigh JS, Elliott MA. T1rho contrast in functional magnetic resonance imaging. *Magn Reson Med* 2005;54:1155-62.

4. Gonyea JV, Watts R, Applebee A, Andrews T, Hipko S, Nickerson JP, Thornton L, Filippi CG. In vivo quantitative whole-brain T1 rho MRI of multiple sclerosis. *J Magn Reson Imaging* 2015;42:1623-30.
5. Heo HY, Wemmie JA, Johnson CP, Thedens DR, Magnotta VA. Eccentricity mapping of the human visual cortex to evaluate temporal dynamics of functional T1 ρ mapping. *J Cereb Blood Flow Metab.* 2015;35:1213-9.
6. Haris M, Yadav SK, Rizwan A, Singh A, Cai K, Kaura D, Wang E, Davatzikos C, Trojanowski JQ, Melhem ER, Marincola FM, Borthakur A. T1rho MRI and CSF biomarkers in diagnosis of Alzheimer's disease. *Neuroimage Clin.* 2015;7:598-604.
7. Johnson CP, Follmer RL, Oguz I, Warren LA, Christensen GE, Fiedorowicz JG, Magnotta VA, Wemmie JA. Quantitative T1 ρ mapping links the cerebellum and lithium use in bipolar disorder. *Mol Psychiatry* 2015;20:149. doi: 10.1038/mp.2015.10.
8. Johnson CP, Follmer RL, Oguz I, Warren LA, Christensen GE, Fiedorowicz JG, Magnotta VA, Wemmie JA. Brain abnormalities in bipolar disorder detected by quantitative T1 ρ mapping. *Mol Psychiatry* 2015;20:201-6.
9. Andronesi OC, Bhat H, Reuter M, Mukherjee S, Caravan P, Rosen BR. Whole brain mapping of water pools and molecular dynamics with rotating frame MR relaxation using gradient modulated low-power adiabatic pulses. *Neuroimage* 2014;89:92-109.
10. Mangia S, Carpenter AF, Tyan AE, Eberly LE, Garwood M, Michaeli S. Magnetization transfer and adiabatic T1 ρ MRI reveal abnormalities in normal-appearing white matter of subjects with multiple sclerosis. *Mult Scler.* 2013;20:1066-1073.
11. Haris M, McArdle E, Fenty M, Singh A, Davatzikos C, Trojanowski JQ, Melhem ER, Clark CM, Borthakur A. Early marker for Alzheimer's disease: hippocampus T1rho estimation. *J Magn Reson Imaging* 2009; 29: 1008–12.
12. Haris M, Singh A, Cai K, Davatzikos C, Trojanowski JQ, Melhem ER, Clark CM, Borthakur A. T1rho (T1 ρ) MR imaging in Alzheimer's disease and Parkinson's disease with and without dementia. *J Neurol* 2011;258:380–385.

13. Nestrasil I, Michaeli S, Liimatainen T, Rydeen CE, Kotz CM, Nixon JP, Hanson T, Tuite PJ. T1rho and T2rho MRI in the evaluation of Parkinson's disease. *J Neurol* 2010; 257: 964–8.
14. Yuan J, Zhou J, Ahuja AT, Wang YX. MR chemical exchange imaging with spin-lock technique (CESL): a theoretical analysis of the Z-spectrum using a two-pool R(1rho) relaxation model beyond the fast-exchange limit. *Phys Med Biol* 2012; 57: 8185–200
15. Yuan J, Zhao F, Chan Q, Wang YX. Observation of biexponential T(1rho) relaxation of in-vivo rat muscles at 3T. *Acta Radiol* 2012;53:675-81.
16. Zaiss M, Bachert P. Chemical exchange saturation transfer (CEST) and MR Z-spectroscopy in vivo: a review of theoretical approaches and methods. *Phys Med Biol*. 2013;58:R221-69.
17. Vinogradov E, Sherry AD, Lenkinski RE. CEST: from basic principles to applications, challenges and opportunities. *J Magn Reson*. 2013;229:155-72.
18. Chen SZ, Yuan J, Deng M, Wei J, Zhou J, Wang YX. Chemical exchange saturation transfer (CEST) MR technique for in-vivo liver imaging at 3.0 tesla. *Eur Radiol*. 2016;26:1792-800.
19. Deng M, Chen SZ, Yuan J, Chan Q, Zhou J, Wang YX. Chemical Exchange Saturation Transfer (CEST) MR Technique for Liver Imaging at 3.0 Tesla: an Evaluation of Different Offset Number and an After-Meal and Over-Night-Fast Comparison. *Mol Imaging Biol*. 2016;18:274-82.
20. Wang YX. Medical imaging in pharmaceutical clinical trials: what radiologists should know. *Clin Radiol* 2005;60:1051-7.
21. Yuan J, Zhao F, Griffith JF, Chan Q, Wang YX. Optimized efficient liver T(1rho) mapping using limited spin lock times. *Phys Med Biol* 2012;57:1631-40.
22. Wang YX, Zhao F, Yuan J, Mok GS, Ahuja AT, Griffith JF. Accelerated T1rho relaxation quantification in intervertebral disc using limited spin-lock times. *Quant Imaging Med Surg* 2013;3:54-8.

23. Zhu Y, Zhang Q, Liu Q, Wang YX, Liu X, Zheng H, Liang D, Yuan J. PANDA- T1p: Integrating principal component analysis and dictionary learning for fast T1p mapping. *Magn Reson Med* 2015;73:263-72.
24. Yuan J, Li Y, Zhao F, Chan Q, Ahuja AT, Wang YX. Quantification of T(1p) relaxation by using rotary echo spin-lock pulses in the presence of B(0) inhomogeneity. *Phys Med Biol* 2012;57:5003-16.
25. Johnson CP, Thedens DR, Magnotta VA. Precision-guided sampling schedules for efficient T1p mapping. *J Magn Reson Imaging* 2015; 41, 242-50.
26. Li Y, Zhao F, Wang YX, Ahuja AT, Yuan J. Study of magnetization evolution by using composite spin-lock pulses for T1p imaging. *Conf Proc IEEE Eng Med Biol Soc* 2012;2012:408-11.
27. Chen W. Errors in quantitative T1rho imaging and the correction methods. *Quant Imaging Med Surg* 2015; 5, 583-91.
28. Cai K, Singh A, Poptani H, et al. CEST signal at 2ppm (CEST@2ppm) from Z-spectral fitting correlates with creatine distribution in brain tumor. *NMR Biomed* 2015; 28, 1-8
29. Chen W, Chan Q, Wang YX. Breathhold black blood quantitative t1rho imaging of liver using single shot fast spin echo acquisition. *Quant Imaging Med Surg* 2016;6(2):168-177.
30. Casula V, Autio J, Nissi MJ, Auerbach EJ, Ellermann J, Lammentausta E, Nieminen MT. Validation and optimization of adiabatic T1p and T2p for quantitative imaging of articular cartilage at 3 T. *Magn Reson Med*. 2016 Mar 4. doi: 10.1002/mrm.26183.
31. Vymazal J, Righini A, Brooks RA, Canesi M, Mariani C, Leonardi M, Pezzoli G. T1 and T2 in the brain of healthy subjects, patients with Parkinson disease, and patients with multiple system atrophy: relation to iron content. *Radiology* 1999;211:489-495.
32. Neema M, Goldberg-Zimring D, Guss ZD, Healy BC, Guttmann CR, Houtchens MK, Weiner HL, Horsfield MA, Hackney DB, Alsop DC, Bakshi R. 3 T MRI relaxometry detects T2 prolongation in the cerebral normal-appearing white matter in multiple sclerosis. *Neuroimage* 2009;46:633-641.

33. Siemonsen S, Finsterbusch J, Matschke J, Lorenzen A, Ding XQ, Fiehler J. Age-dependent normal values of T2* and T29 in brain parenchyma. *Am J Neuroradiol* 2008; 29: 950–955.
34. Ding XQ, Kucinski T, Wittkugel O, Goebell E, Grzyska U, Görg M, Kohlschütter A, Zeumer H. Normal brain maturation characterized with age-related T2 relaxation times: an attempt to develop a quantitative imaging measure for clinical use. *Invest Radiol* 2004; 39: 740–746.
35. Hasan KM, Walimuni IS, Kramer LA, Frye RE. Human brain atlas based volumetry and relaxometry: application to healthy development and natural aging. *Magn Reson Med* 2010; 64: 1382–1389
36. Wang J, Shaffer ML, Eslinger PJ, Sun X, Weitekamp CW, Patel MM, Dossick D, Gill DJ, Connor JR, Yang QX. Maturation and aging effects on human brain apparent transverse relaxation. *PLoS One*. 2012;7:e31907
37. Borthakur A, Sochor M, Davatzikos C, Trojanowski JQ, Clark CM. T1rho MRI of Alzheimer's disease. *Neuroimage* 2008;41: 1199–1205
38. Watts R, Andrews T, Hipko S, Gonyea JV, Filippi CG. In vivo whole-brain T1-rho mapping across adulthood: normative values and age dependence. *J Magn Reson Imaging* 2014; 40: 376–82.
39. Drayer BP. Imaging of the aging brain. Part I. Normal findings. *Radiology* 1988; 166:785-96
40. Wong EC, Liu TT, Luh WM, Frank LR, Buxton RB. T1 and T2 selective method for improved SNR in CSF-attenuated imaging: T2-FLAIR. *Magn Reson Med*. 2001;45(3):529-32.
41. Charagundla SR, Borthakur A, Leigh JS, Reddy R. Artifacts in T1p-weighted imaging: correction with a self-compensating spin-locking pulse. *J Magn Reson* 2003;162(1):113-21.

42. Ashburner J, Friston K. *Image segmentation*. In: Frackowiak R, Friston K, Frith C, Dolan R, Price C, Zeki S, Ashburner J, Penny W, eds *Human brain function*, 2nd ed. Academic, 2003 San Diego, pp 695–706
43. Ashburner J, Friston KJ. Unified segmentation. *Neuroimage* 2005;26:839–851.
44. Ashburner J, Friston KJ. Nonlinear spatial normalization using basis functions. *Hum Brain Mapp* 1999;7:254–266.
45. Tzourio-Mazoyer N, Landeau B, Papathanassiou D, Crivello F, Etard O, Delcroix N, Mazoyer B, Joliot M. Automated anatomical labeling of activations in SPM using a macroscopic anatomical parcellation of the MNI MRI single-subject brain. *Neuroimage* 2002;15:273-89.
46. Song XW, Dong ZY, Long XY, Li SF, Zuo XN, Zhu CZ, He Y, Yan CG, Feng Zang YF. REST: A Toolkit for Resting-State Functional Magnetic Resonance Imaging Data Processing. *PLoS ONE* 2011; 6: e25031.
47. Wang YX, He GX, Tong GH, Wang DB, Xu KY. Cerebral asymmetry in a selected Chinese population. *Australasian Radiology* 1999;43:321-324
48. Ge Y, Grossman RI, Babb JS, Rabin ML, Mannon LJ, Kolson DL. Age-related total gray matter and white matter changes in normal adult brain. Part I: volumetric MR imaging analysis. *Am J Neuroradiol.* 2002;23:1327-33.
49. Miller AK, Alston RL, Corsellis JA. Variation with age in the volumes of grey and white matter in the cerebral hemispheres of man: measurements with an image analyser. *Neuropathol Appl Neurobiol.* 1980;6:119-32.
50. Plaschke K, Frauenknecht K, Sommer C, Heiland S. A single systemic transient hypotension induces long-term changes in rats' MRI parameters and behavior: relation to aging. *Neurol Res.* 2009;31:304-12.
51. Zhao F, Yuan J, Lu G, Zhang LH, Chen ZY, Wáng YX. T1ρ relaxation time in brain regions increases with ageing: an experimental MRI observation in rats. *Br J Radiol.* 2016;89:20140704

Fig Legends

Figure 1: Brain gray matters T1 ρ relaxation (Y-axis: msec.) vs. age (X-axis: years). a: amygdala; b: caudate; c: cortices; d: hippocampus; e: pallidum; f: putamen; g: thalamus; h: global gray matter.

Figure 2. Box-plot of T1 ρ at various gray matter structures. A regional difference shows hippocampus and amygdala have the highest measurement, while pallidum and putamen the lowest measurement. Y-axis: T1 ρ value at msec. * & ^o: outlier measurements.

Supplements

Supplement document 1: A comparison of ROI-based and voxel-wised Data Analysis

Supplement document 2: Polynomial fitting for grey matter T1 ρ value vs. age

Supplement document 3: Supplement Table 1. Descriptive Statistics, Correlation with Age for T1 ρ value of global WM, GM and selected gray matter structure with linear regression fit.

Figure
[Click here to download high resolution image](#)

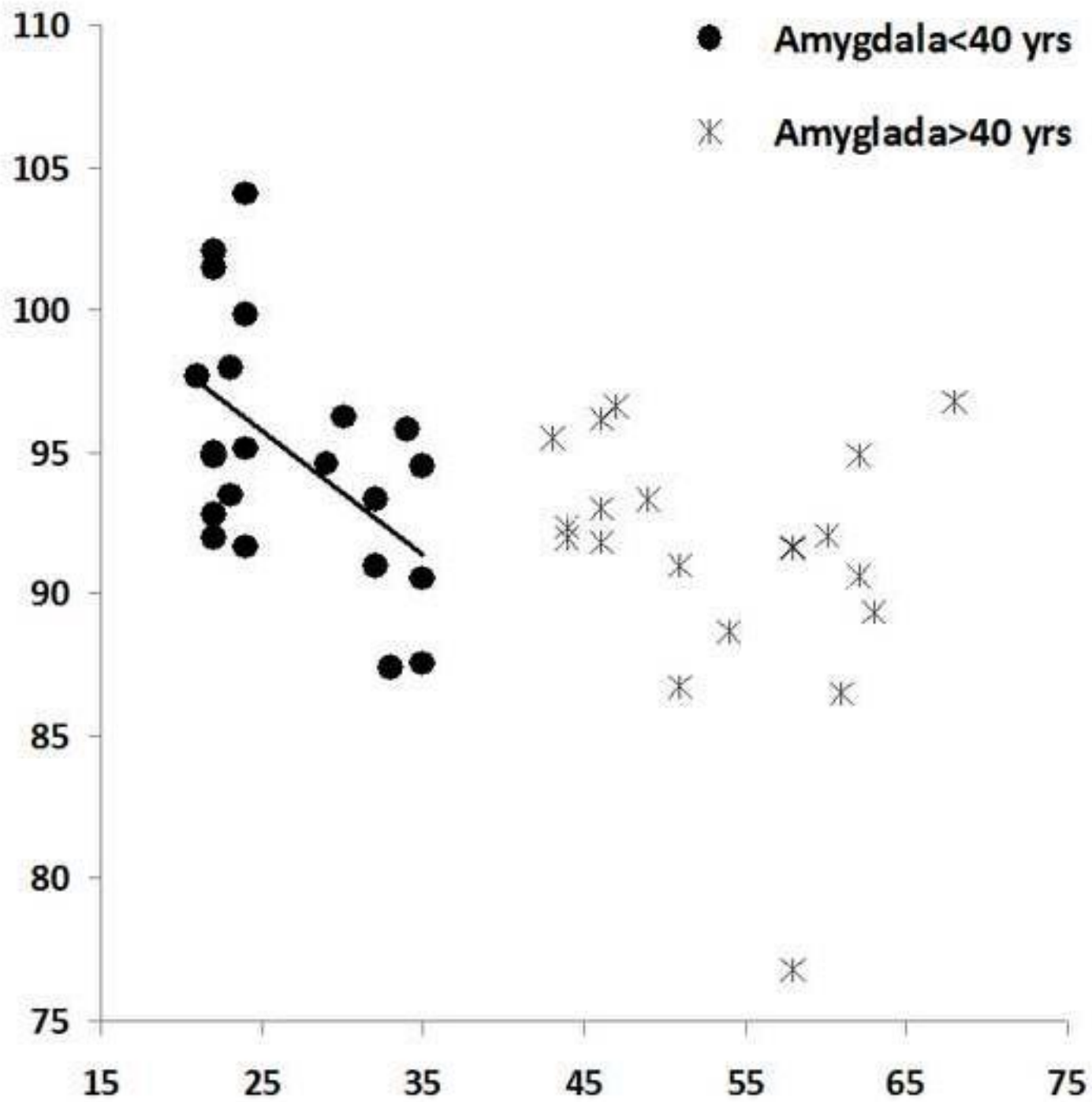


Figure
[Click here to download high resolution image](#)

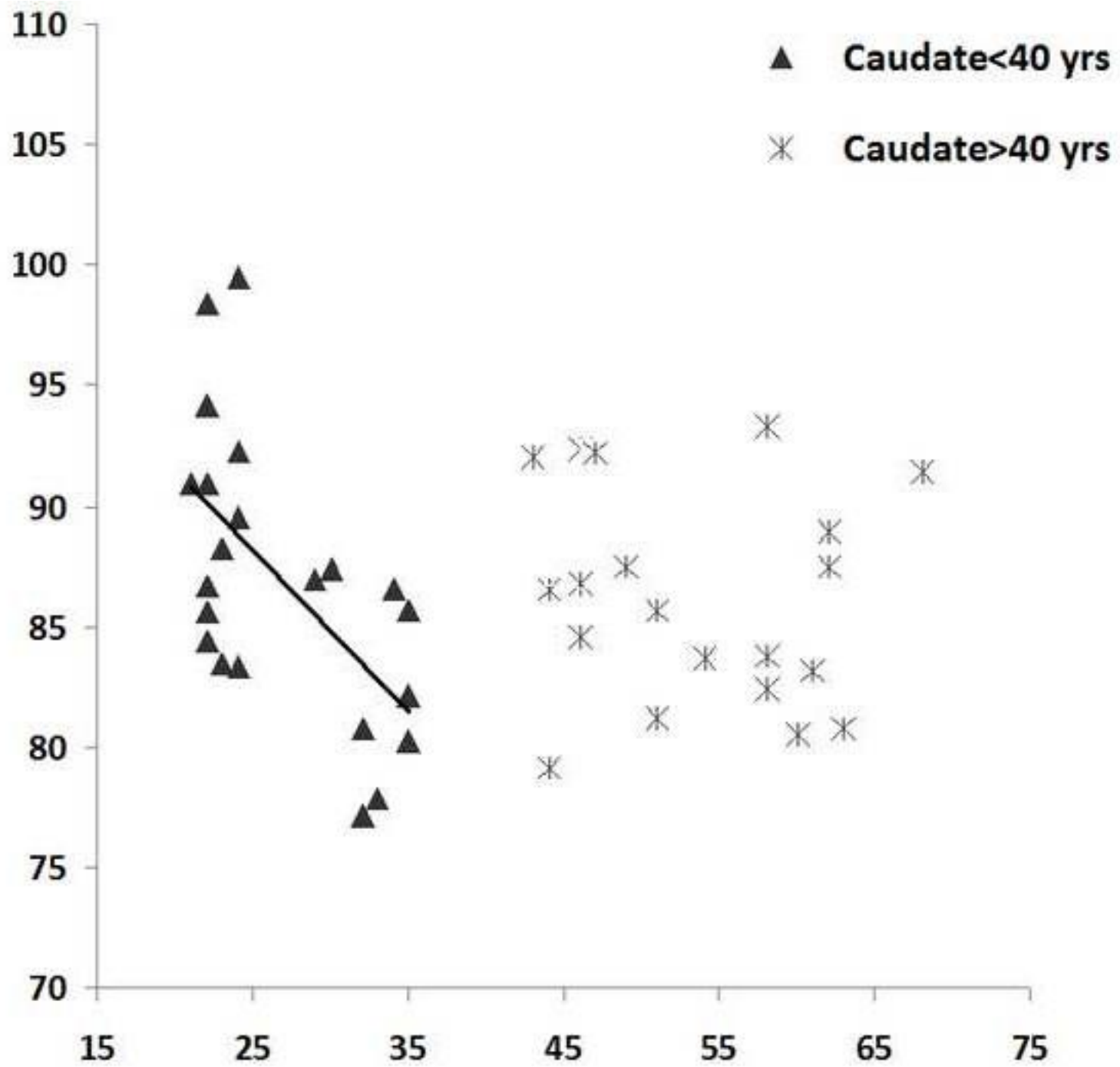


Figure
[Click here to download high resolution image](#)

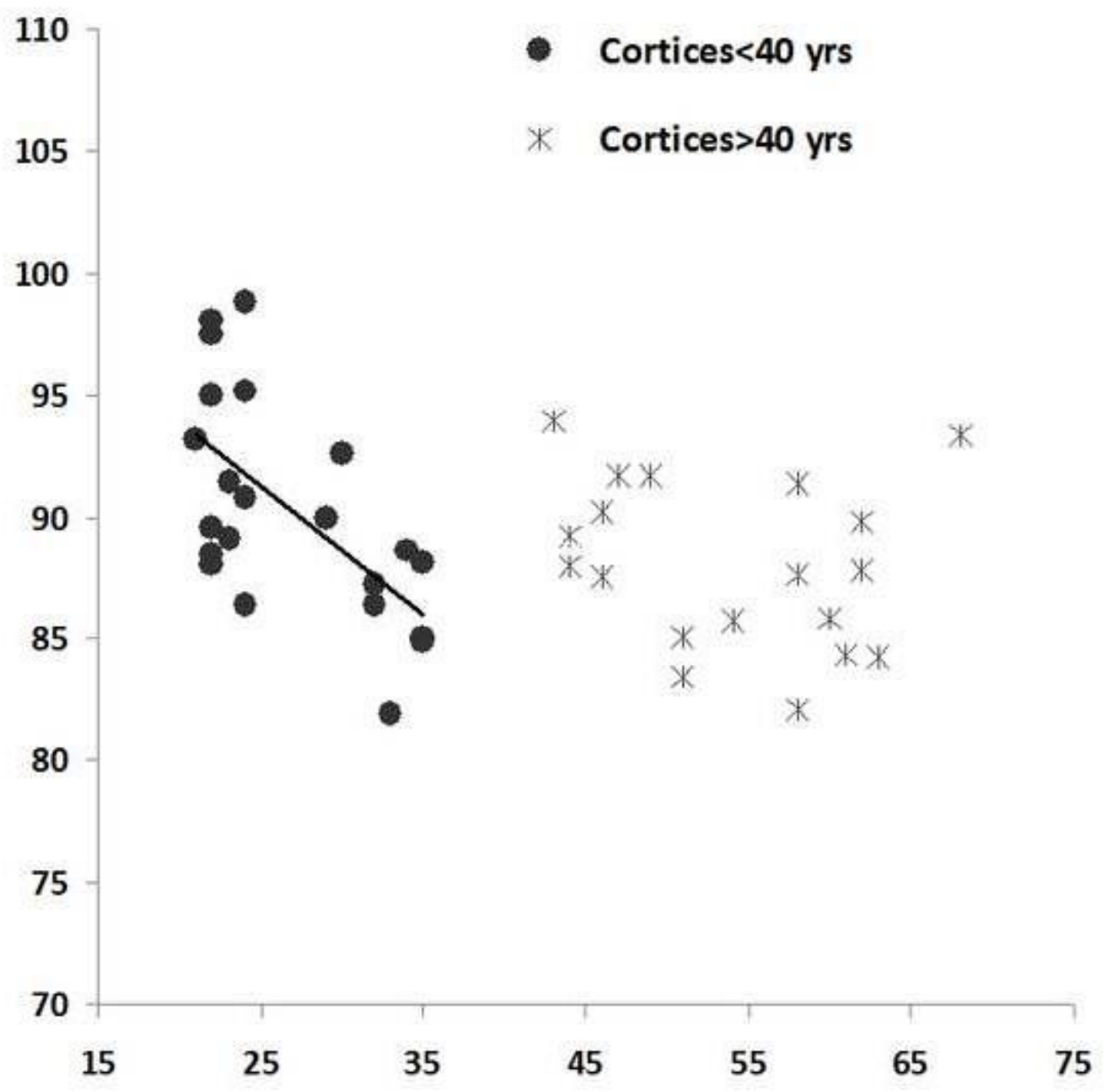


Figure
[Click here to download high resolution image](#)

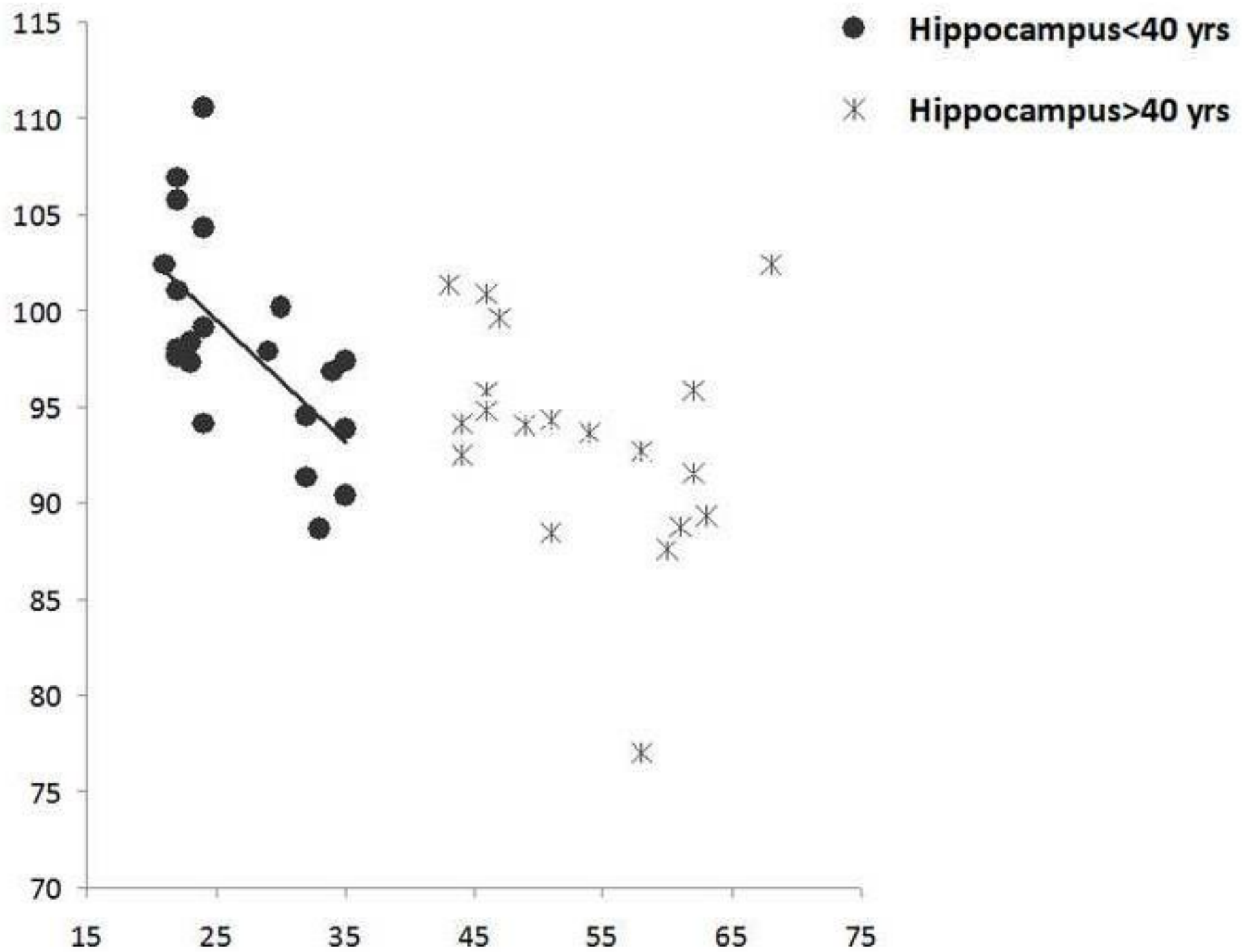


Figure
[Click here to download high resolution image](#)

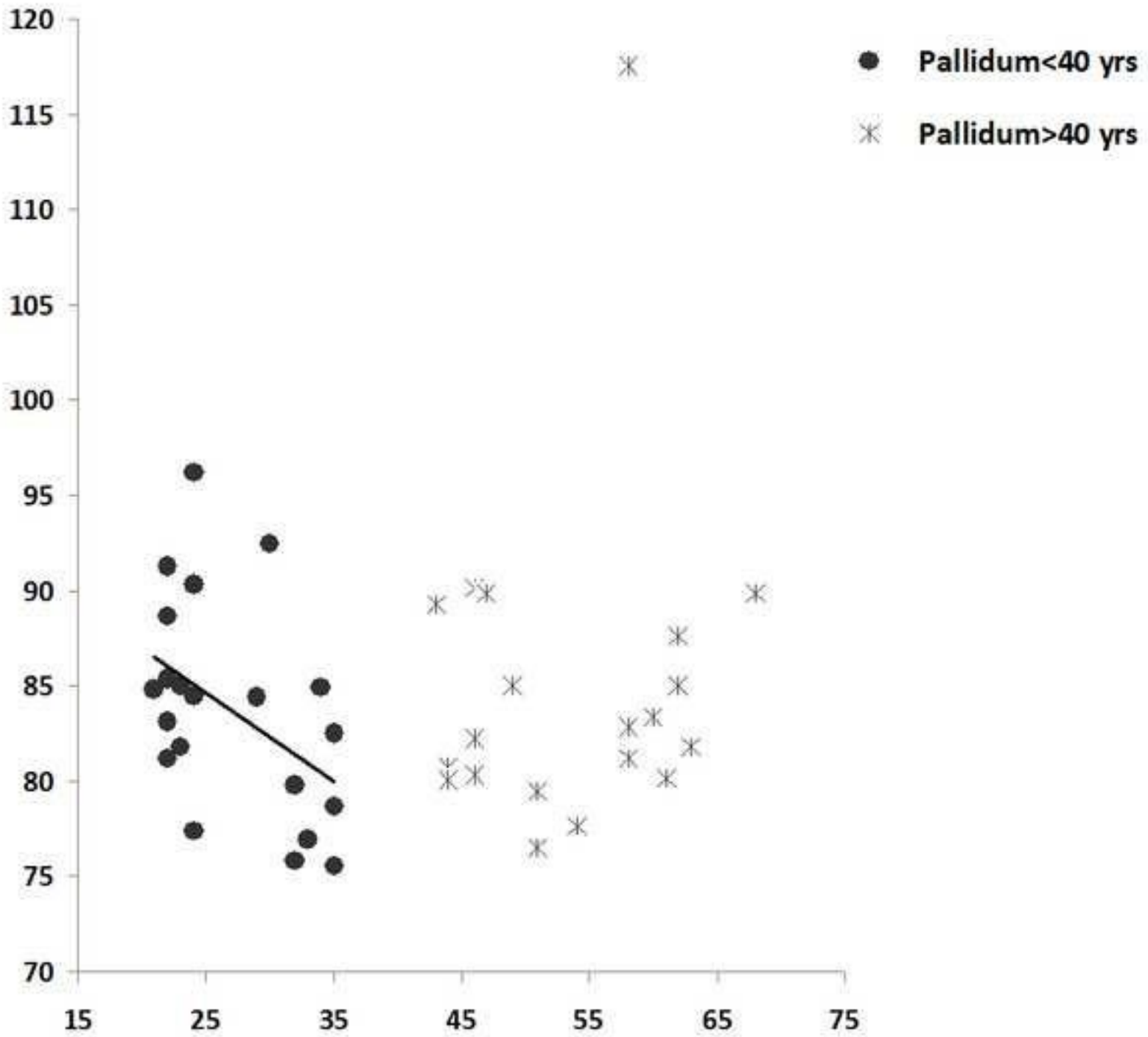


Figure
[Click here to download high resolution image](#)

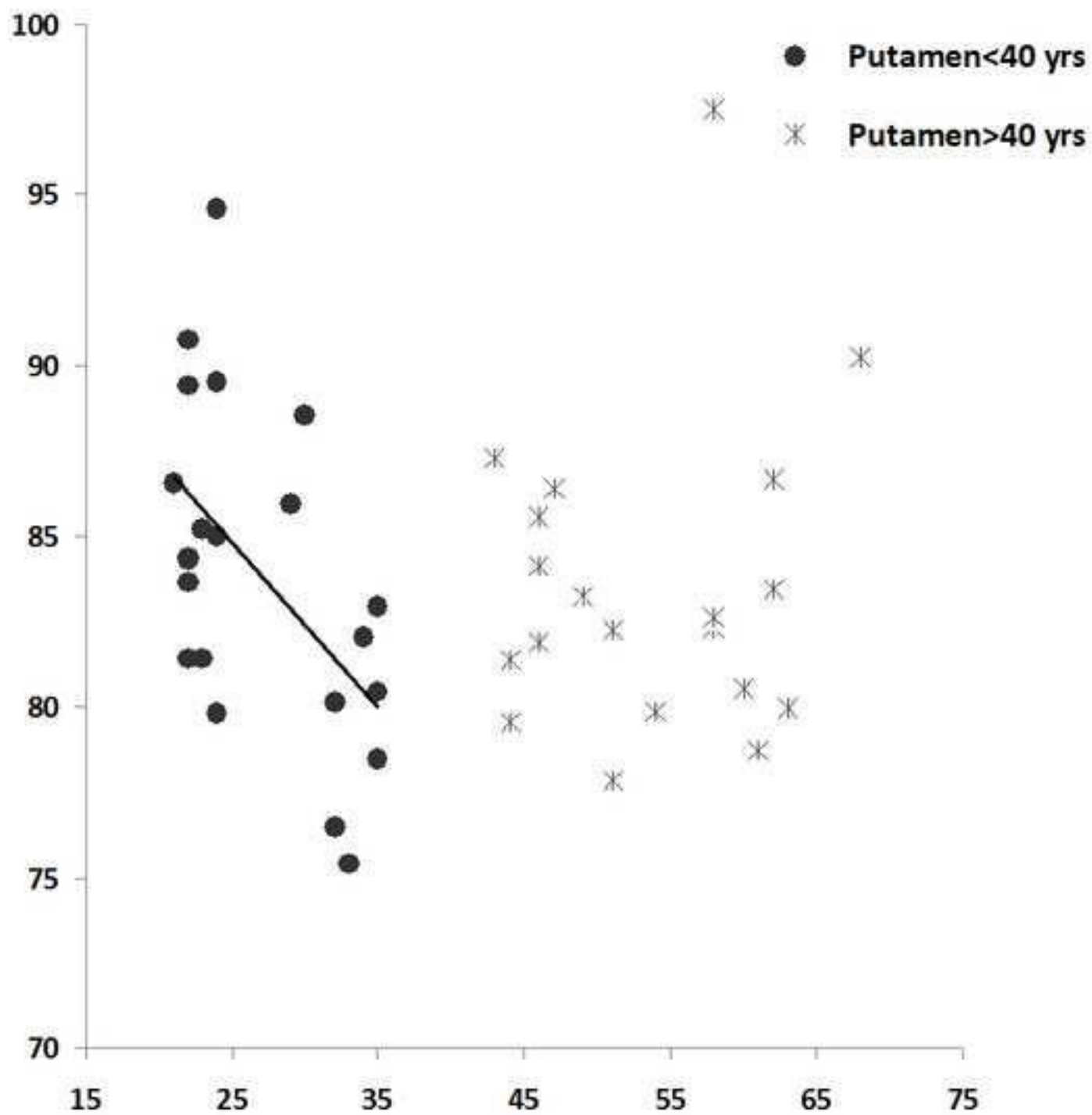


Figure
[Click here to download high resolution image](#)

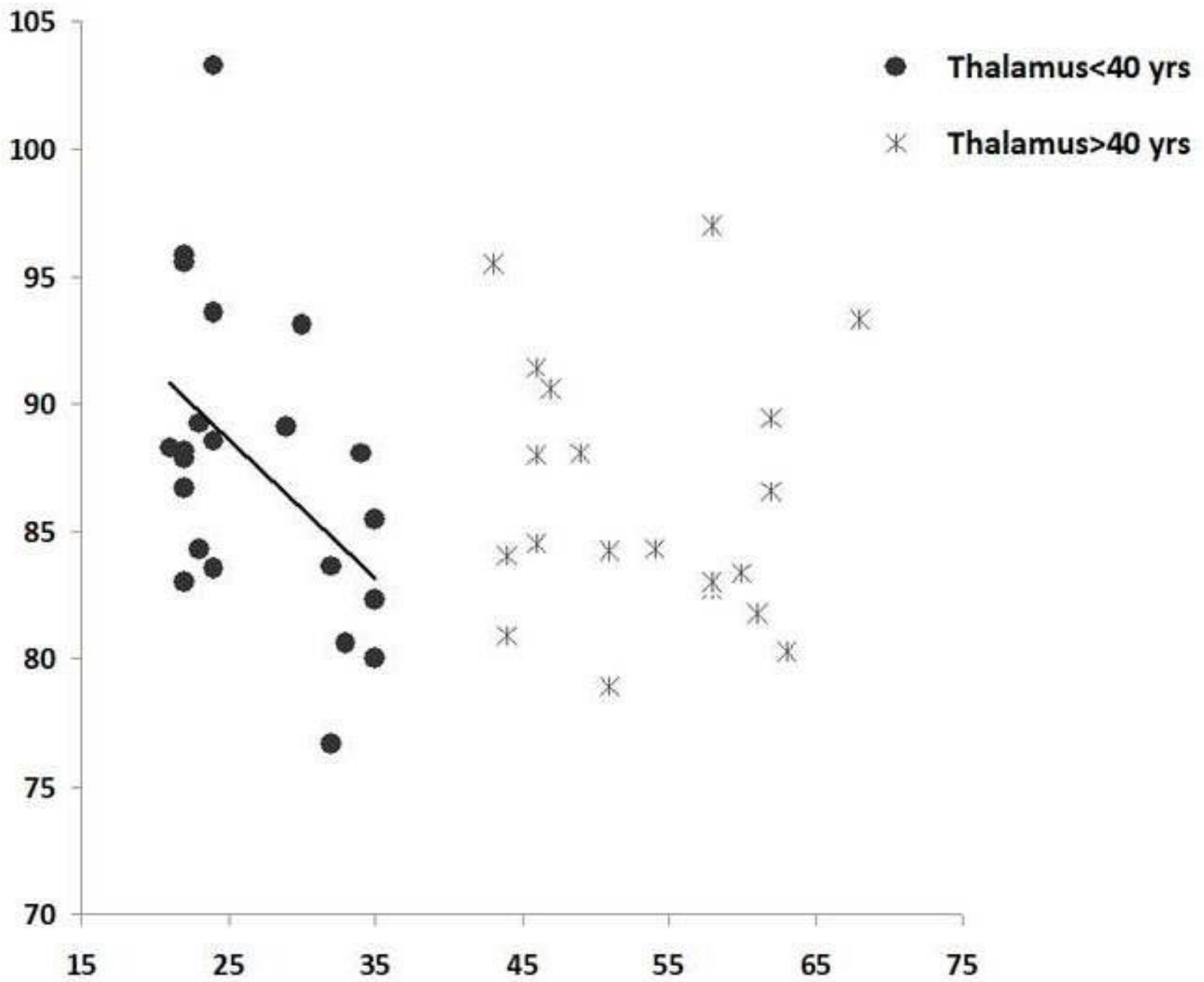


Figure
[Click here to download high resolution image](#)

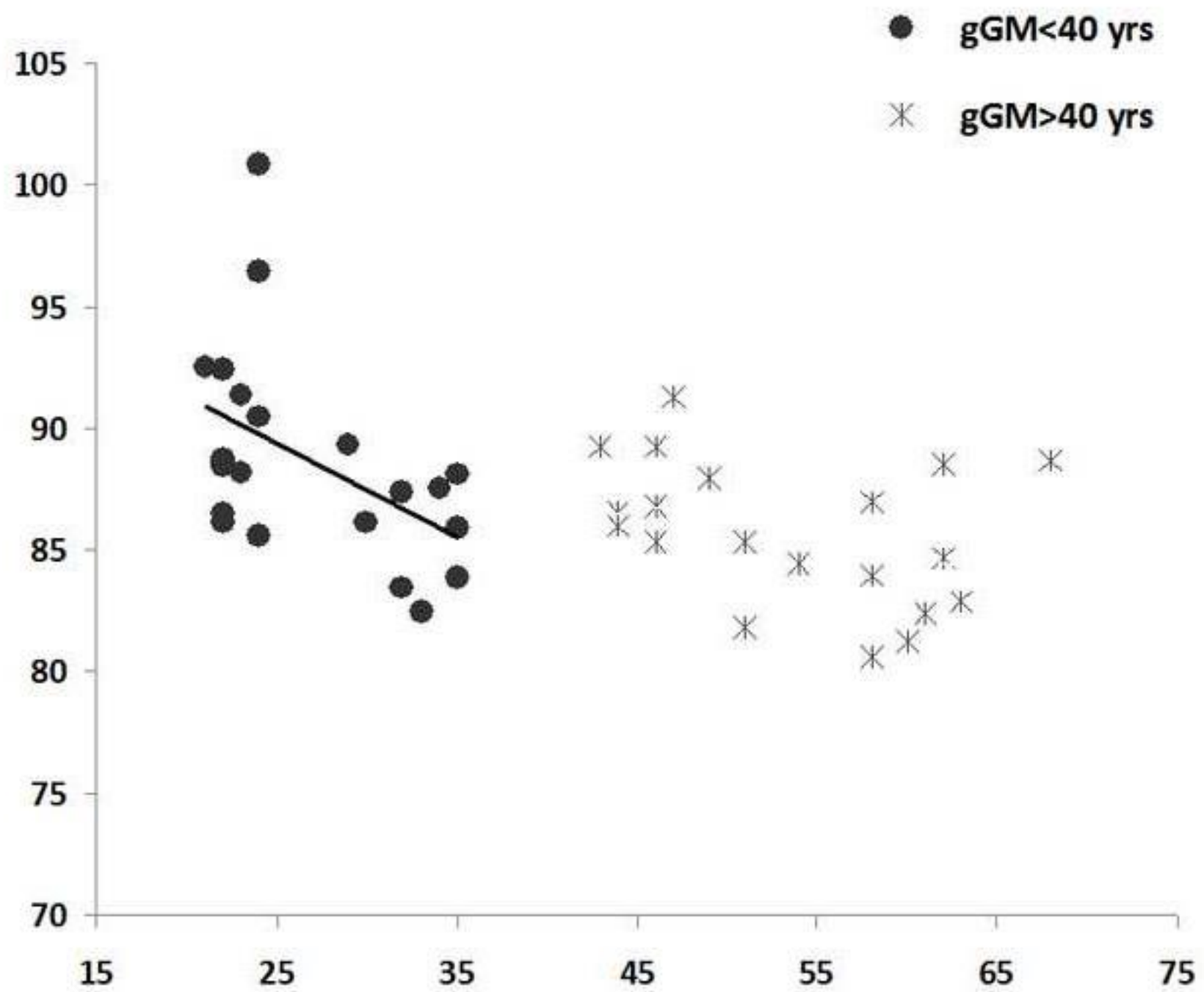


Figure
[Click here to download high resolution image](#)

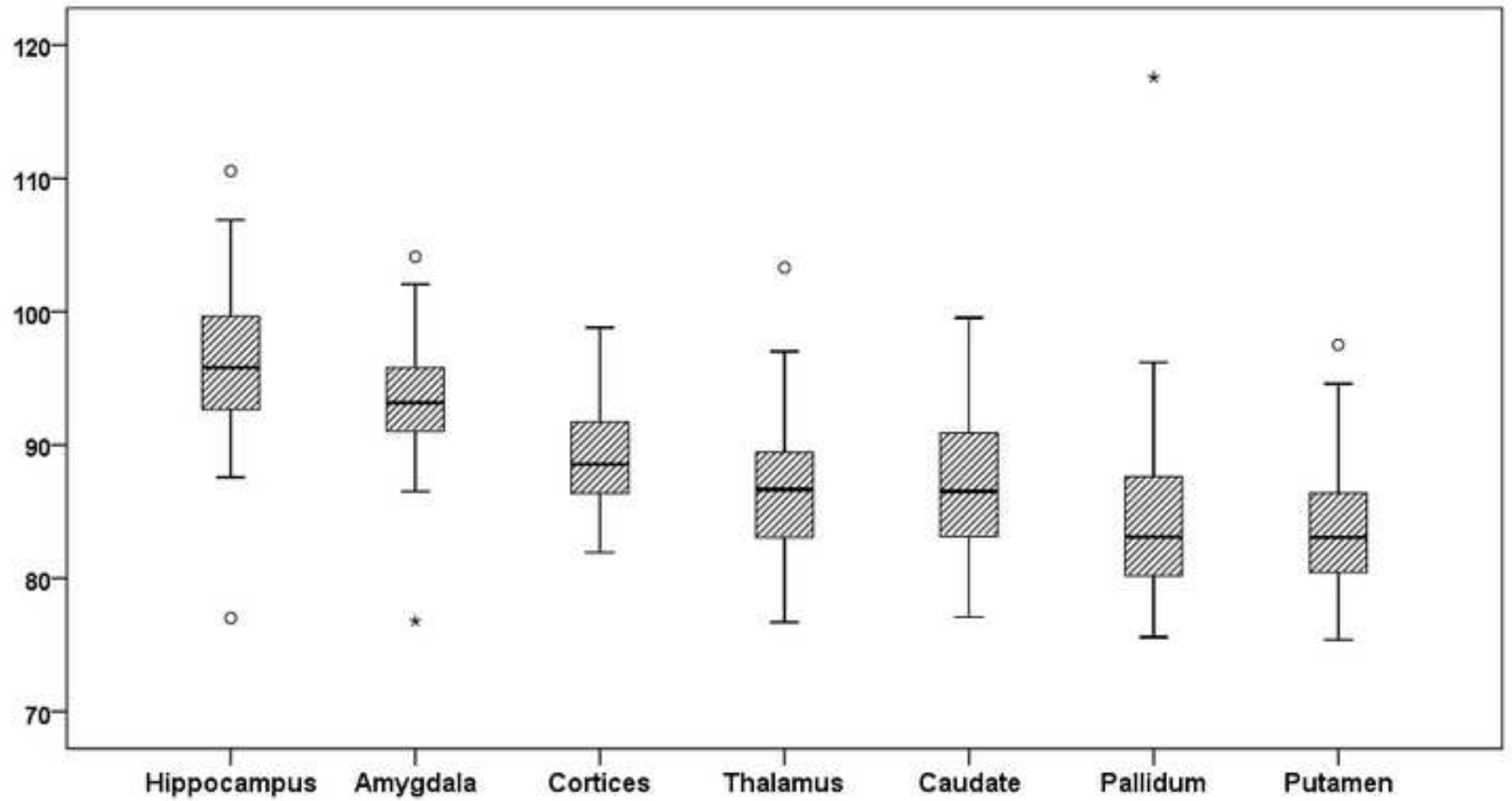


Table 1: Descriptive Statistics, Regression and Correlation with Age for T1p value of global gray matter (gGM) and selected GM structures in younger-than-40-year group

Structure	Mean	SD	Regression coefficient with age		Correlation	P value
			slope	R square		
Amygdala*	94.95	4.34	-0.19	0.026	-0.533	0.011
Caudate*	86.90	5.91	-0.32	0.017	-0.601	0.030
Cortices**	90.29	4.53	-0.21	0.014	-0.621	0.002
Hippocampus**	98.37	5.37	-0.33	0.097	-0.625	0.002
Pallidum*	83.81	5.49	-0.15	0.098	-0.449	0.036
Putamen*	83.93	4.76	-0.23	0.005	-0.537	0.010
Thalamus*	87.60	6.06	-0.23	0.036	-0.478	0.024
gGM*	88.66	4.22	-0.39	0.239	-0.489	0.021

Mean: T1p value in msec; SD: standard deviation, * p<0.05; p<0.005

Table2: Descriptive Statistics, Regression and Correlation with Age for T1p value of global gray matter (gGM) and selected GM structures in older-than-40-year group

Structure	Mean	SD	Regression coefficient with age		Correlation	P value
			slope	R square		
Amygdala	91.37	4.51	-0.04	0.102	-0.231	0.328
Caudate	86.15	4.43	-0.05	0.145	-0.099	0.678
Cortices	88.03	3.37	-0.04	0.140	-0.213	0.368
Hippocampus	93.38	5.73	-0.14	0.171	-0.301	0.198
Pallidum	85.03	8.72	0.1	0.019	0.153	0.519
Putamen	83.57	4.56	0.02	0.131	0.144	0.545
Thalamus	86.42	5.11	-0.1	0.083	-0.050	0.834
gGM	85.70	2.97	-0.14	0.142	-0.375	0.103

Mean: T1p value in msec, SD: standard deviation